Preparation of Iron-cobalt-cerium Heterogeneous Nano-catalysts to Produce Light Hydrocarbons from Synthesis Gas

H.A. Hashemzehi[a], A.A. Mirzaei[a], H. Atashi[b] and F. Rezaeian[b]

[a]*Department of Chemistry, Faculty of Sciences, University of Sistan and Baluchestan, P. O. Box: 98135-674, Zahedan, Iran*
[b]*Department of Chemical Engineering, Faculty of Engineering, University of Sistan and Baluchestan, P. O. Box: 98164-161, Zahedan, Iran*

Nowadays, due to the decline in oil supplies and raising the price of petroleum, countries have been led to other sources of fuel and energy. In this respect, the use of methods such as the production of light hydrocarbons from synthesis gas is highly regarded by the Fischer-Tropsch process. This process is performed by heterogeneous catalysts consisting of two parts; a catalyst support (generally porous and made of silica), and an active phase (generally made of metal). In fact, the catalyst is the heart of Fischer-Tropsch process. In this study, iron-cobalt-cerium tri-metallic nano-catalyst based on silica was prepared by the wet impregnation method. The catalyst was tested in a fixed bed microreactor and a wide range of products was analyzed by GC technique. The results show that by increasing temperature, the CO conversion is increased and the efficiency of products is improved. Finally, the structure of nano-catalyst was characterized using the techniques of scanning electron microscopy (SEM), Brunauer-Emmett-Teller (BET), X-ray diffraction (XRD) and temperature programed-reduction (TPR) to realize the particle size and surface properties of the catalyst.

Keywords: Nano-catalyst, Light hydrocarbons, Synthesis gas, Fischer-Tropsch synthesis, Wet impregnation

INTRODUCTION

The most important section of the Fischer Tropsch synthesis (FTS) is its catalytic section. The catalytic function can play a significant role in this process. There are generally two components in a catalyst: support of catalyst and active phase. In fact, the active phase is the major component responsible for the catalytic activity. The active phase of the catalyst is the same solid or metal that shows the special catalytic features for doing the reaction. In fact, the solid catalysts have been composed of the active centers placed on the outer surface of the catalyst. Metals such as iron, cobalt, nickel, *etc.* are used as the active phase in the FT catalyst [1].

The FTS is a process in which synthesis gas (a mixture of carbon monoxide and hydrogen) produced from natural gas or coal is converted into linear hydrocarbons and oxygenated products [2,3]. The most important catalysts employed in the FTS are the compounds and complexes composed of group VIIIB metals in the periodic table, which are used either as single metallic or bi-metallic catalysts [4]. Among them, the catalysts based on iron, cobalt, and ruthenium have been more considered and many studies have been conducted accordingly [5,6].

Iron catalysts are mainly prepared by co-precipitation method and also as bimetallic catalysts using potassium or copper metal as a second component that enhances the performance of Fe metal. In addition, oxides such as Al_2O_3 and SiO_2 are employed as a carrier or support for these catalysts. It is worth noting that these catalysts have a high activity for gas-water displacement reaction and are flexible over the different ratios of H_2/CO and so active for the small ratios of H_2/CO [7,8].

Nickel catalyst is the most appropriate option in terms of

---

*Corresponding author. E-mail: h.ateshy@hamoon.usb.ac.ir

Washing gel with distilled water about 7-8 times   Final shape of silica support

Fig. 1. Fabrication method of silica support.
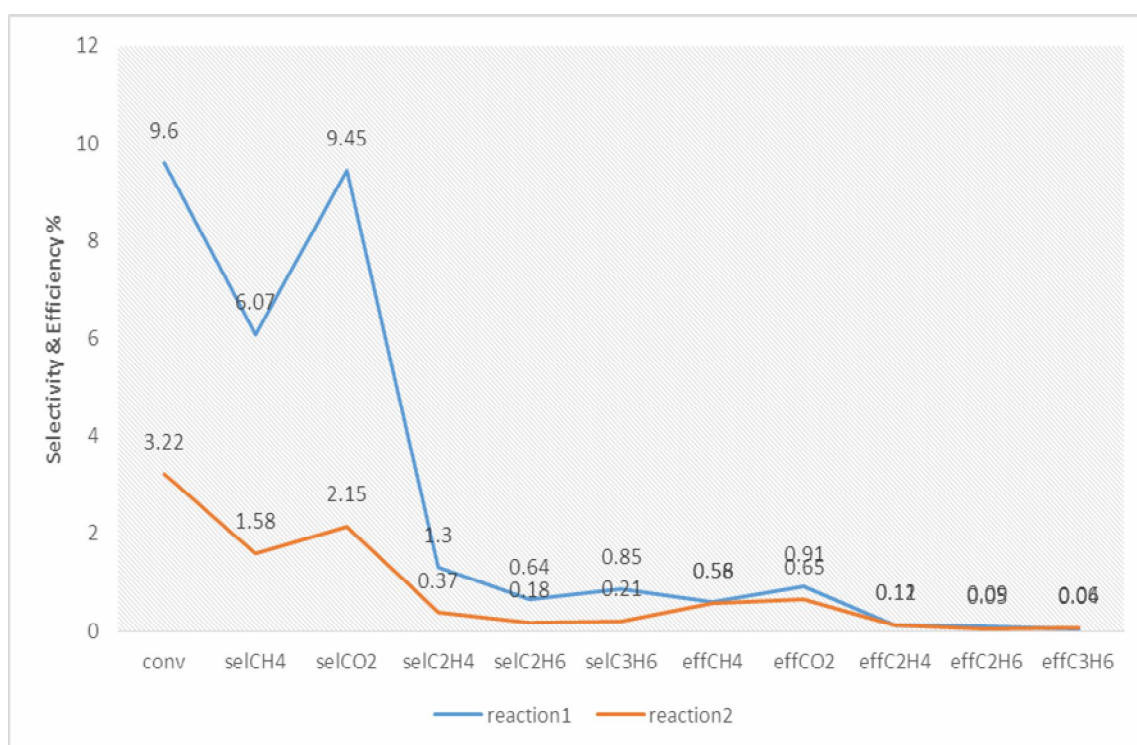
Fig. 2. The results of catalyst testing under the reaction operating conditions.

the high hydrogenation capacity in the FT process and production of hydrocarbons with high molecular weight [9]. The use of this catalyst leads to the decrease of temperature required for the reduction reaction making the nickel catalyst an enhancing agent under specific conditions [10]. The major drawback is that nickel catalyst is converted into nickel carbonyl form at high pressures and, as a result, the restriction on the pressure limits the FT reaction. In addition, since the selectivity of methane in the presence of nickel is high and generally, methane is an undesirable product, this catalyst is not appropriate [11].

Cerium metal and especially its oxide (CeO_2) have many applications. For example, they can be used in the manufacture of ceramic electrolyte in fuel cells. However, among various applications, the catalytic activity of cerium is very significant since it can be used as a catalyst in the metallic state and as a catalyst support in the metal oxide state. Cerium catalysts are those of the FT catalysts used to produce the hydrocarbons with higher molecular weight and fuels. In the case of the fuels produced by cerium catalyst, it is worth mentioning that they could reduce the pollutions *via* the decrease of impurities and outputs such as NO_X.
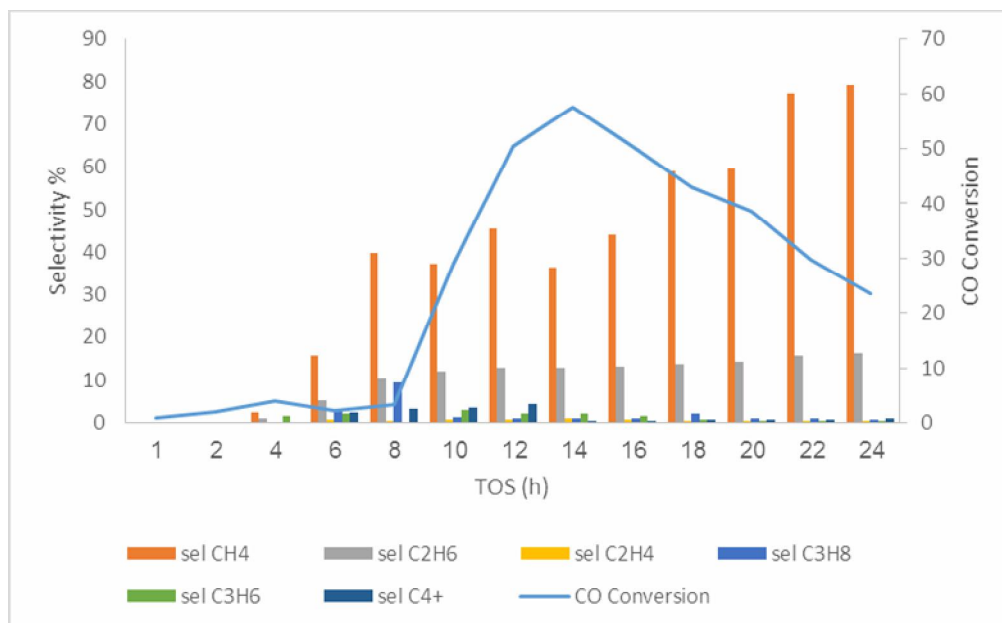
Fig. 3. Hydrocarbon selectivity and CO Conversion over time on stream.

However, the main disadvantage of this catalyst is its high price [12,13].

In this article, the wet impregnation method is used for iron-cobalt-cerium heterogeneous nano-catalysts. In this method, the goal is to fill up the pores by the metal salt solution with sufficient concentration in the range of nano to increase the reaction rate, decrease the reaction time, and reduce the energy consumption, and produce of products with higher productivity and selectivity.

EXPERIMENTAL

Silica Support Fabrication

3-4 drops of phenolphthalein solution were added to 20% sodium silicate solution (an aqueous solution with high viscosity) until the change of color, from colorless to purple. Then, 1 M HCl solution was added dropwise during 30 min (the value of HCl solution added during this period of time was about 50 ml). After addition of acid to the medium, the solution became colorless and a gel was produced. Then, the resulting solution was stirred at 500 rpm for 8 h with an electric mixer. In the next step, the obtained gel was rinsed with lots of distilled water about 7-8 times to remove interfering sodium ions and dried in the oven at 120 °C for

20 h, and then, calcined at 600 °C for 4 h. The resulting material was finally obtained as the powder. Figure 1 shows the fabrication method of silica.

Preparation of {30%w (Fe-Ce-Co)/70%w SiO₂} Tri-metallic Catalyst by Wet Impregnation Method

In this method, the catalyst was prepared based on the ratio of its components. In this ratio, the support and each of the metals included 70%w and 10%w of the catalyst, respectively. The salts of $(Co(NO_3)_2.6H_2O)$, $(Ce(NO_3)_3.6H_2O)$ and $(Fe(NO_3)_3.9H_2O)$ were used as precursors for Co, Ce and Fe metals. The calculations were performed based on 3 g of catalyst. 1.489, 0.929 and 2.164 g of $(Co(NO_3)_2.6H_2O)$, $(Ce(NO_3)_3.6H_2O)$ and $(Fe(NO_3)_3.9H_2O)$ were mixed together with a rotary balloon, and then 2.1 g of catalyst support (silica) was added to it (fast wetting). After turning on the rotary device, impregnation process was performed at 80 °C and at a constant speed of 20 rpm during 8 hours. Then, the catalyst was removed from the rotary balloon, filtered by a vacuum pump and dried in the oven at 120 °C for 4 h. Finally, the catalyst was calcined at 600 °C for 4 h. At this stage, the catalyst was ready for the reactor testing.
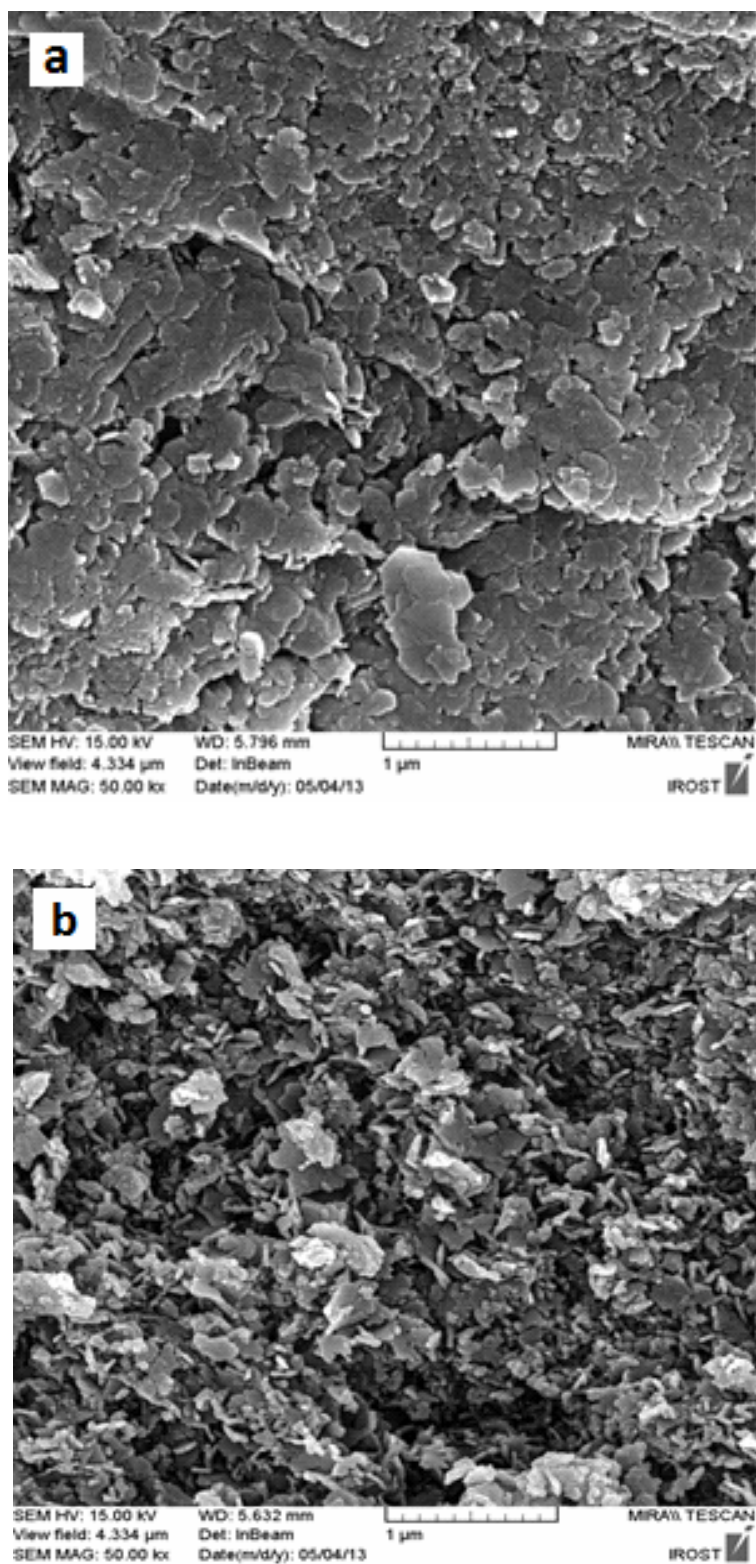
Fig. 4. SEM images of precursor (a) and calcined catalyst before (b) and after (c) reactor testing.
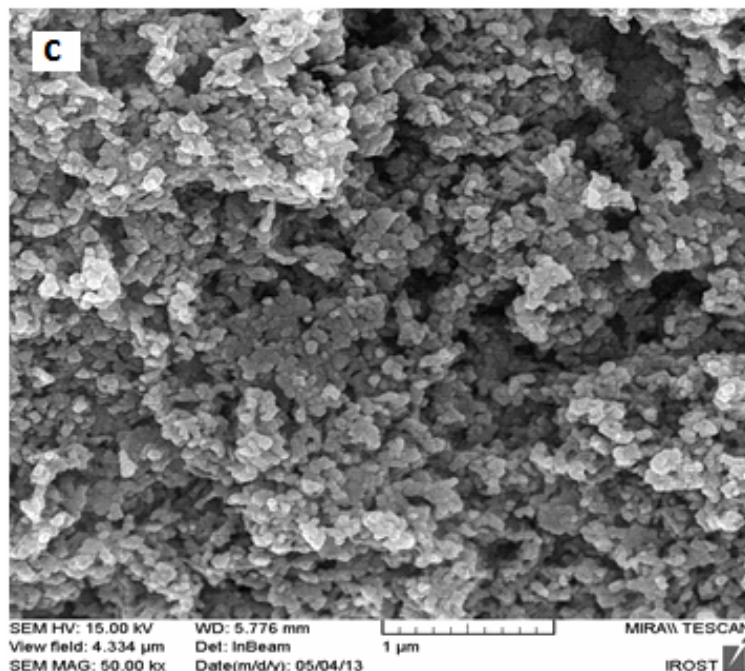
Fig. 4. Continued.

The Reaction Operating Conditions

The first reaction condition was done at temperature of 300 (°C), pressure of 4 bar and input gases ratio of 1:1. The second reaction condition was done at temperature of 350 (°C), pressure of 4 bar and input gases ratio of 1:1.

RESULTS AND DISCUSSIONS

To evaluate the efficiency of the catalyst, 1 g of the related catalyst was placed in a laboratory fixed bed micro-reactor. Then, in order to perform the reaction, the reactor temperature was adjusted to the desired temperature, the carbon monoxide gas valve was opened and the flow rate ratio of input gases (feed) was set by the control panel. After passing the required time for the reaction, gas chromatography instrument was turned on and the obtained products were analyzed to determine the conversion percent of carbon monoxide gas and selectivity with respect to each of the products.

The Results of Catalyst Testing under the Reaction Operating Conditions

The results obtained from the GC analysis are shown in Fig. 2. As can be seen in Fig. 2, CO and H_2 gases were converted into a wide range of light hydrocarbons that the efficiency and selectivity for each of them could be calculated. In the case of CO gas conversion percent, the higher conversion percent leads to more catalyst efficiency and selectivity.

As it follows from Fig. 2, the CO conversion percent has been increased and the product's efficiency shows the better performance of the catalyst in higher temperature (350 °C compared to 300 °C). However, it should be noted that the temperatures higher than 350 °C had a negative effect on the catalyst efficiency and conversion percent of CO, because the high temperatures deform the active centers of catalyst and inactivate them. Therefore, the catalyst exhibits the maximum performance at a critical temperature and does not have the favorable efficiency at higher temperatures.

The CO conversion and hydrocarbons selectivity over time on stream were illustrated in Fig. 3. As can be seen in the figure, the paraffin products increased over the time, while the olefin products increased with increasing the CO Conversion. By increasing the CO conversion, ethylene and propylene increased and heavy hydrocarbons decreased.
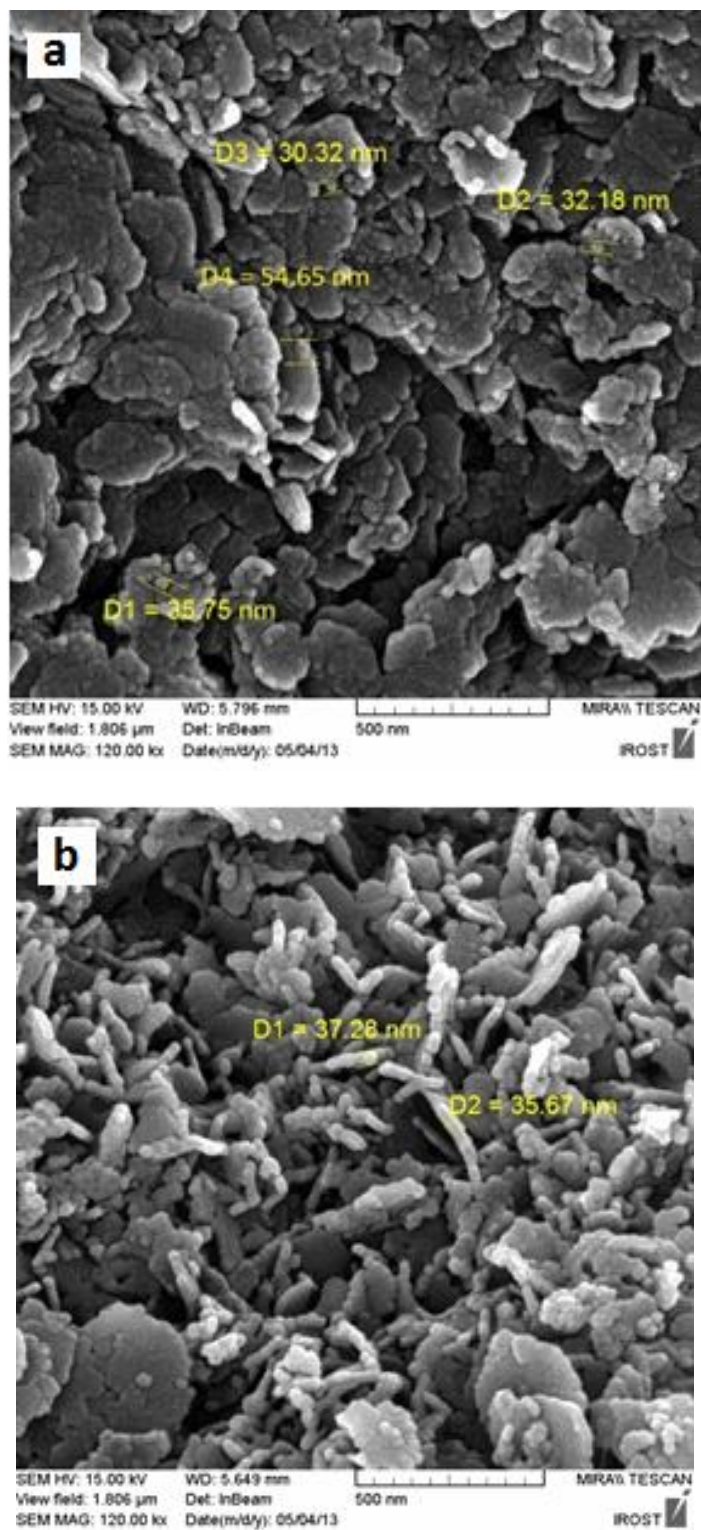
Fig. 5. SEM images with 120000 times magnification for precursor (a), and calcined catalyst before (b) and after (c) reactor testing.
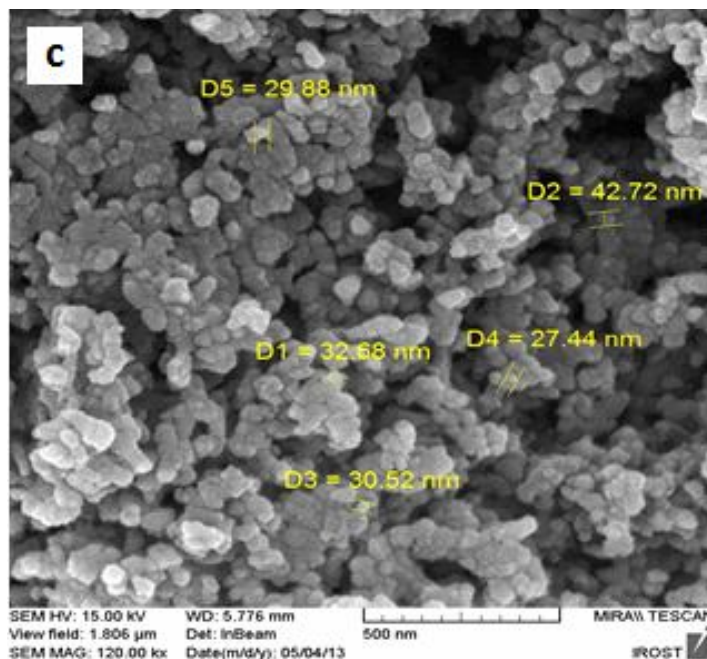
Fig. 5. Continued.

Selectivity of methane increased by increasing the time on stream. Product selectivity is such that with the passage of time, the selectivity of heavy hydrocarbons reduced and the selectivity of methane and light hydrocarbons increased.

Catalyst Characterization

In order to evaluate the texture of optimized catalyst, SEM technique was used. SEM images of precursor and calcined catalyst before and after reactor testing are shown in Fig. 4. This information helps understand the changes of precursor texture during the calcining process and also the changes of catalyst texture during the FT process.

Figure 5 shows SEM images of precursor and calcined catalyst before and after reactor testing with the magnification of 120000 times; that is more than double for images shown in Fig. 4. The size of some particles has been determined in these images.

Based on the SEM images, the catalyst dimensions are in nano-scale. In fact, the synthesized catalyst is a nano-catalyst with many advantages compared to the common counterparts with the larger particle size. For example, nano-catalysts increase the rate and efficiency of chemical reactions more, so that more products can be produced within less time scale. In addition, they are able to save energy.

Figure 6 shows XRD spectrum of the precursor catalyst, the catalyst before the reactor test, and the catalyst after the reactor test. To determine the different phases of the catalyst, the XRD spectrum was used. All catalyst states are amorphous, and the phase cannot be determined.

It is said that over time the carbon formation and deposition of the active sites change the selectivity. Sintering or agglomeration of calcination temperature of 600 °C resulted in a reduction in the reactor test catalyst effective level (SEM results also confirm this phenomenon). In addition, the surface area after the test of the reactor increased due to the formation of carbide and carbon deposits (Table 1). The reason for reducing the surface area is that the catalyst before reactor test was oxide and, the reduction operation is perfumed after reactor test (by H_2 activator) so, the increased surface has occurred in terms of changing the composition (before the reactor is oxide and after the reactor is metal) and this change has increased the catalyst surface area.
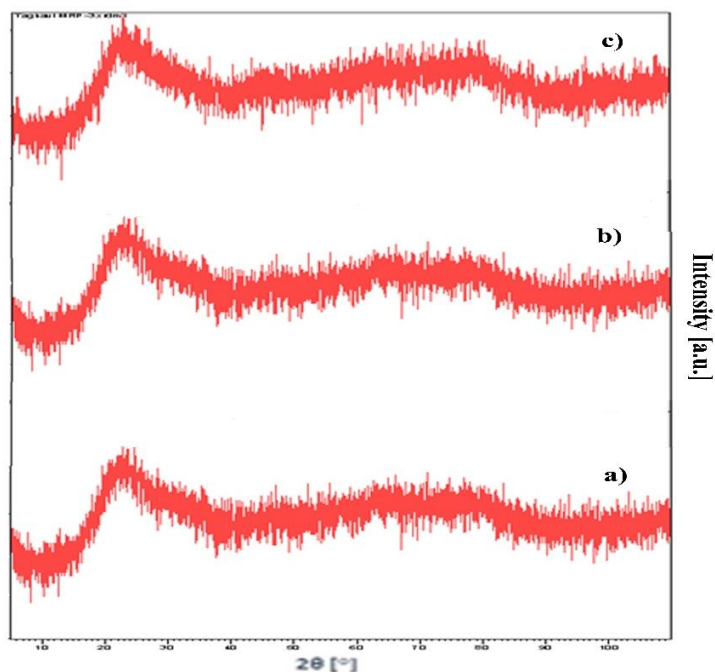
Fig. 6. XRD spectrum of a) the precursor catalyst b) before the reactor test and c) after the reactor test.

Table 1. BET Results for Catalyst

Catalyst	Surface area (m^2 g^{-1})
The precursor catalyst	120.4155
Before the reactor test	110.3132
After reactor test	322.5383

TPR is used to evaluate the reducibility of nanoparticles. Fig. 7 illustrates the TPR profiles of iron-cobalt-cerium heterogeneous nano-catalysts. As can be seen, four peaks of different reductions are shown by TPR profile. According to the literature, reduction of iron-cobalt-cerium oxides occurs in the range of 330-350 °C, 350-600 °C and 485-800 °C, respectively [14,15].

CONCLUSIONS

The use of metal nano-catalysts with the porous substrate in the FT process leads to produce lighter hydrocarbons with high efficiency and selectivity. The obtained results from SEM images, BET, XRD and TPR profile show that the calcination and reactor testing of catalyst affects significantly the texture and structure of the precursor and catalyst. The precursors have the larger particle size, and the calcined catalyst exhibits the accumulation and rather larger size particles after reactor testing compared to those before reactor testing. The synthesized nano-catalyst depicts the higher CO conversion percent at a higher temperature; however, it should be
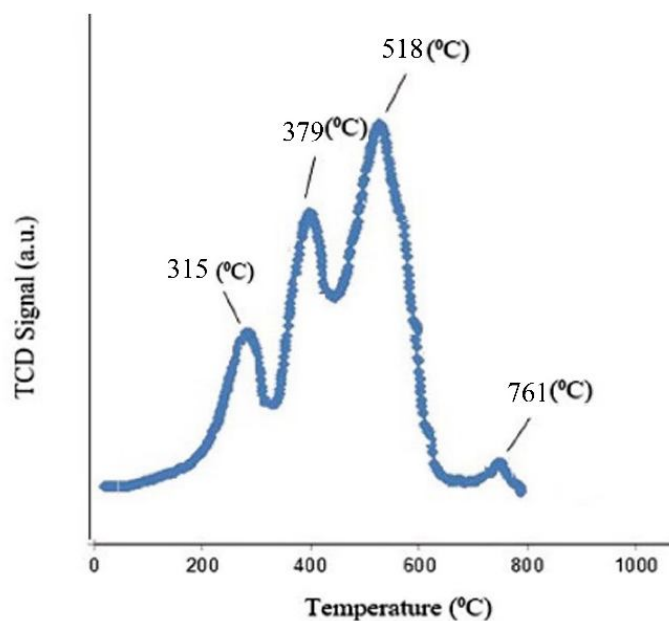
Fig. 7. Temperature‑Programmed Reduction profile for the catalyst.

mentioned that the very high temperatures deactivate the catalyst. Moreover, it is noteworthy that nano-catalysts have several advantages compared to bulk counterparts, including the increase of reaction rate, the decrease of reaction time, reduction of energy consumption, and generation of product with the higher productivity and selectivity.

REFERENCES

[1]   Dry, M. E., The fischer-tropsch process: 1950-2000. *Catal. Today,* **2002**, *71*, 227-241, DOI: 10.1016/S0920-5861(01)00453-9.

[2]   Khorashadizadeh, M.; Atashi, H., Toward the development of a robust kinetic model for the Cobalt Fischer-Tropsch catalyst lifetime using a novel sigmoidal pattern. *Phys. Chem. Res.,* **2018**, *6*, 173-192, DOI: 10.22036/pcr.2017.82484.1369.

[3]   Atashi, H.; Rezaeian, F., Modelling and optimization of Fischer-Tropsch products through iron catalyst in fixed-bed reactor. *Int. J. Hydrogen Energy,* **2017**, *42*, 15497-15506, DOI: 10.1016/j.ijhydene.2017.04.224.

[4]   Seleznev, A.; Petrov, L. A.; Kononenko, V. I.; Chupova, I. A.; Ryabina, A. V., Temperature-programmed reduction of cobalt-containing catalysts

[5]   Schulz, H., Short history and present trends of Fischer–Tropsch synthesis. *Appl. Catal., A,* **1999**, *186*, 3-12, DOI: 10.1016/S0926-860X(99)00160-X.

[6]   Razmjooie, A.; Atashi, H.; Shahraki, F., The application of hybrid RSM/ANN methodology of an iron-based catalyst performance in Fischer-Tropsch synthesis. *Phys. Chem. Res.,* **2017**, *5*, 585-600, DOI: 10.22036/pcr.2017.72773.1346.

[7]   Yu, W.; Wu, B.; Xu, J.; Tao, Zh.; Xiang, H.; Li, Y., Effect of Pt impregnation on a precipitated iron-based Fischer-Tropsch synthesis catalyst. *Catal. Lett.* **2008**, *125*, 116, DOI: 10.1007/s10562-008-9524-3.

[8]   Mirzaei, A. A.; Arsalanfar, M.; Bozorgzadeh, H. R.; Samimi, A., A review of Fischer-Tropsch synthesis on the cobalt based catalysts. *Phys. Chem. Res.,* **2014**, *2*, 179-201, DOI: 10.22036/pcr.2014.5786.

[9]   Cheng-hua, Z.; Yong, Y.; Zhi-chao, T.; Hong-wei, X.; Yong-wang, L., Structural properties and reduction behavior of Ni promoted FeMnK/SiO$_2$ catalysts for Fischer-Tropsch synthesis. *J. Fuel Chem. Tech.,* **2006**,

of the Fischer-Tropsch synthesis based on ultrafine aluminum powders alloyed with rare-earth metals. *Russ. Chem. Bull.,* **2009**, *58*, 1315-1317, DOI: 10.1007/s11172-009-0173-5.

34, 695-699, DOI: 10.1016/S1872-5813(07)60004-8.

[10] Li, G.; Hu, L.; Hill, J. M., Comparison of reducibility and stability of alumina-supported Ni catalysts prepared by impregnation and co-precipitation. *Appl. Catal., A*, **2006**, *301*, 16-24, DOI: 10.1016/j.apcata.2005.11.013.

[11] Adesina, A. A., Hydrocarbon synthesis *via* Fischer-Tropsch reaction: travails and triumphs. *Appl. Catal., A*, **1996**, *138*, 345-367, DOI: 10.1016/0926-860X(95)00307-X.

[12] Zhang, X.; Su, H.; Zhang,Y.; Gu, X., Effect of CeO_2 promotion on the catalytic performance of Co/ZrO_2 catalysts for Fischer-Tropsch synthesis. *Fuel.* **2016**, *184*, 162-168, DOI: 10.1016/j.fuel.2016.06.125.

[13] Mirzaei, A. A.; Arsalanfar, M.; Ebrahimzadeh, F.; Atashi, H.; Mirhoseini Moghaddam, S. H., Kinetic study of Fischer Tropsch synthesis over co precipitated iron-cerium catalyst. *Phys. Chem. Res.,* **2013**, *1*, 69-80, DOI: 10.22036/pcr.2013.2641.

[14] Davies, K. J.; Wells, S.; Charles, S. W.; The effect of temperature and oleate adsorption on the growth of maghemite particles. *J Magn Magn Mater.,* **1993**, *122*, 24-28, DOI:10.1016/0304-8853(93)91031-2.

[15] Khan, A.; Smirniotis, P. G., Relationship between temperature-programmed reduction profile and activity of modified ferrite-based catalysts for WGS reaction. *J Mol Catal A,* **2008**, *280*, 43-51, DOI: 10.1016/j.molcata.2007.10.022.